

# Combining Ultracentrifugation and Peptide Termini Group-specific Immunoprecipitation for Multiplex Plasma Protein Analysis<sup>§</sup>

Sonja Volk<sup>‡§</sup>, Thomas D. Schreiber<sup>‡§</sup>, David Eisen<sup>‡§</sup>, Calvin Wiese<sup>¶</sup>, Hannes Planatscher<sup>‡</sup>, Christopher J. Pynn<sup>‡||</sup>, Dieter Stoll<sup>‡||</sup>, Markus F. Templin<sup>‡</sup>, Thomas O. Joos<sup>‡</sup>, and Oliver Pötz<sup>‡\*\*</sup>

Blood plasma is a valuable source of potential biomarkers. However, its complexity and the huge dynamic concentration range of its constituents complicate its analysis. To tackle this problem, an immunoprecipitation strategy was employed using antibodies directed against short terminal epitope tags (triple X proteomics antibodies), which allow the enrichment of groups of signature peptides derived from trypsin-digested plasma. Isolated signature peptides are subsequently detected using MALDI-TOF/TOF mass spectrometry. Sensitivity of the immunoaffinity approach was, however, compromised by the presence of contaminant peaks derived from the peptides of nontargeted high abundant proteins. A closer analysis of the enrichment strategy revealed nonspecific peptide binding to the solid phase affinity matrix as the major source of the contaminating peptides. We therefore implemented a sucrose density gradient ultracentrifugation separation step into the procedure. This yielded a 99% depletion of contaminating peptides from a sucrose fraction containing 70% of the peptide-antibody complexes and enabled the detection of the previously undetected low abundance protein filamin-A. Assessment of this novel approach using 15 different triple X proteomics antibodies demonstrated a more consistent detection of a greater number of targeted peptides and a significant reduction in the intensity of nonspecific peptides. Ultracentrifugation coupled with immunoaffinity MS approaches presents a powerful tool for multiplexed plasma protein analysis without the requirement for demanding liquid chromatography separation techniques. *Molecular & Cellular Proteomics* 11: 10.1074/mcp.O111.015438, 1–14, 2012.

The identification of reliable biomarkers in health and disease has gained considerable interest in recent years (1). In

From the <sup>‡</sup>NMI Natural and Medical Sciences Institute at the University of Tübingen, 72770 Reutlingen, Germany, and <sup>¶</sup>Wellspring Clinical Lab, Inc., Altamonte Springs, Florida 32701, and the <sup>||</sup>University of Applied Sciences Albstadt-Sigmaringen, 72488 Sigmaringen, Germany

Received October 28, 2011, and in revised form, April 16, 2012

Published, MCP Papers in Press, April 23, 2012, DOI 10.1074/mcp.O111.015438

many ways, blood plasma is the ideal sample in which to search for them. Not only is it readily available and easy to collect, but it also contains a huge number of different proteins resulting from both active secretion and cell and tissue leakage from the many tissues with which it comes into contact. These include those responsible for coagulation, immune defense, protein transport, and protease inhibition, the levels of which can provide an indication of an individual's health status (2). The identification and validation of novel plasma-derived protein biomarkers is, however, complicated by the enormous complexity and concentration range of the plasma proteome, which spans more than 10 orders of magnitude (3). MS is a useful tool for the identification of novel biomarkers, capable of providing unambiguous protein assignments. However, limitations imposed by the various ionization processes impact on both the complexity and dynamic range of analytes measurable. A solution to this problem involves the removal of albumin and other highly abundant proteins using immunoaffinity columns (4–7), yet nonspecific depletion of proteins not targeted by the immunoaffinity columns has been reported (8), and depletion efficiency and reproducibility has been found to vary with increasing column use (9–11). Alternatively, sample complexity can be reduced by extensive fractionation using multidimensional separation methods such as two-dimensional PAGE or multidimensional liquid chromatography (12, 13), but such methods are limited by low sample throughput, insufficient sensitivity, unreliability, and cost (14). In contrast, group-specific fractionation of peptides from complex samples has been successfully implemented in a variety of applications such as enrichment of, for example, cysteine-containing or glycosylated peptides (15, 16). Nevertheless, such approaches are limited to the detection of peptides carrying a distinct modification. For targeted issues, peptide-specific antibodies are used for peptide-specific enrichment of tryptically digested proteins. Immunoprecipitates are typically analyzed by highly selective mass spectrometry approaches such as multiple reaction monitoring and quantification of these signature peptides achieved using stable isotope dilution (17, 18). These immunoaffinity-MS approaches have the advantage of relatively high sensitivity and

specificity and can be semiautomated, enabling medium sample throughput (19). Although such approaches have proven capable of isolating peptides derived from clinically relevant plasma proteins (20, 21), they are limited by the availability of appropriate capture antibodies for the proteins and peptides of interest. The requirement of one specific antibody for each analyte is very costly, and the generation of a new antibody for each new marker of interest is time-consuming. Recently published group-specific affinity enrichment strategies could circumvent this problem (22, 23). The triple X proteomics approach employs group-specific antibodies directed against short terminal epitopes (3–4 amino acids) at the N or C terminus of tryptically digested peptides (22) followed by identification of the different captured peptides using tandem MS. As previously demonstrated, this approach enables the efficient enrichment of groups of targeted analytes in cell lysates while reducing the sample complexity sufficiently for fast tandem MS-based peptide identification (24). We therefore investigated the suitability of this TXP<sup>1</sup> immunoaffinity approach to the analysis of nondepleted plasma digest samples.

Matrices applied in immunoaffinity workflows such as protein G beads are prone to nonspecific peptides binding (8, 25). This has been addressed in approaches employing elaborate washing procedures, such as the “magnetic bead trap” prototype. Here, protein G-bound antibody-peptide immunocomplexes are cleansed by applying a counterflow (25). As an alternative we investigated a strategy employing an in-solution separation of antibody-peptide complexes from the remaining digest. In 1934, Theodor Svedberg (26) reported the in-solution separation of molecules with different molecular weights using ultracentrifugation. Nearly another 40 years passed before Tengerdy and Faust (27) applied this technique to the separation of antigen-antibody complexes from unbound antigens, and in 1984, Rødahl *et al.* (28) used an ultracentrifugation procedure to isolate autoimmune complexes from serum. We decided to revisit the idea of using ultracentrifugation to separate peptides bound to TXP antibodies from residual nontargeted peptides in plasma protein digests. 15 TXP antibodies targeted against N- or C-terminal 4–5-amino acid epitopes of plasma proteins differing in their abundances were evaluated using MALDI-TOF/TOF mass spectrometry. Our findings support the use of ultracentrifugation as a fractionation tool for immunoaffinity enrichment MALDI-mass spectrometry-based human plasma proteomics.

### EXPERIMENTAL PROCEDURES

**Generation and Characterization of Anti-peptide Antibodies**—Polyclonal rabbit antibodies were generated and purified as previously described (24). Binding affinities of the purified polyclonal monospecific antibodies were determined using a competitive immunoassay modified after the method of Friguet *et al.* (29, 30). For this purpose,

<sup>1</sup> The abbreviations used are: TXP, triple X proteomics; Doa, 8-amino-3,6-dioxo-octanoic acid; HA, hemagglutinin; PE, phycoerythrin.

the peptide antigens were immobilized to color-coded beads as previously described (24, 31). 400 pg of antibody were preincubated with a 12-step serial dilution of the soluble peptide antigen ranging from 5  $\mu$ M down to 80 pM in 0.1% Tween, PBS for 60 min at room temperature. 500 peptide-coupled beads were added and incubated for additional 60 min. Noncomplexed antibody was detected by incubation with PE-labeled anti-rabbit antibody (2.5  $\mu$ g/ml; Jackson ImmunoResearch, West Grove, PA). The median bead type-specific fluorescence was determined with a Luminex FlexMap 3D system by measuring 100 bead events. As a mean of affinity, the half-maximal effective concentration (EC<sub>50</sub>) of the peptide was calculated using a four-parametric logarithmic fit.

**Isotopically Labeled Peptide Standards**—The vitamin K-dependent protein S peptide NIPGDFECECEPEGYR<sup>\*</sup> containing an <sup>13</sup>C/<sup>15</sup>N isotopically labeled arginine was purchased from Intavis (Cologne, Germany). The increase in mass from the unlabeled NIPGDFECECEPEGYR was 10 Da. The peptide stock concentration was determined by amino acid analysis at Medizinisches Proteom-Center (Bochum, Germany).

**Blood Plasma Collection**—Blood was drawn from the senior author; he had fasted for 10 h, and blood was collected by venous puncture using a 21-gauge Safety Multifly® 0.8 mm/19 mm needle (Sarstedt, Nümbrecht, Germany). A total of 30 ml of blood was collected in four 7.5 ml plasma lithium-heparin S-Monovette® tubes (Sarstedt). Immediately following blood collection and mixing with heparin in the tubes, the samples were centrifuged at room temperature for 10 min at 4000 rpm using a Rotanta/RP5094 rotor (Hettich, Tuttlingen, Germany) to pellet the cells. Plasma supernatant was collected immediately after centrifugation, transferred into 1.5 ml Eppendorf tubes in 60  $\mu$ l/tube aliquots, and stored at –80 °C for 2–4 months. Total elapsed time from collection to storage was 1 h. The experiments were performed according to German law and the Declaration of Helsinki asserted by the institutional ethical committee (Ethik-Kommission der Medizinischen Fakultät und am Universitätsklinikum Tübingen).

**Preparation of Tryptic Plasma Digests**—Tryptic plasma digests were prepared by diluting 60  $\mu$ l of whole plasma with 540  $\mu$ l of 50 mM triethanolamine, pH 8.5. 30  $\mu$ l of 10% *n*-octyl- $\beta$ -D-glucopyranoside solution and 3  $\mu$ l of the reducing agent tris(2-carboxyethyl)phosphine (1 M) were added. The samples were denatured for 5 min at 100 °C. After cooling to room temperature, the samples were alkylated with 6.6  $\mu$ l of 1 M iodoacetamide at room temperature in the dark for 30 min. 100  $\mu$ g of modified Trypsin Gold, mass spectrometry grade (Promega, Madison, WI) was resuspended in 100  $\mu$ l of 50 mM acetic acid. 98  $\mu$ l of the resuspended trypsin was added to the alkylated plasma samples (substrate:enzyme ratio 40:1). Digestion was carried out for 16 h at 37 °C with continuous mixing (650 rpm) in a Thermomixer (Eppendorf, Hamburg, Germany). Trypsin activity was stopped by heating the sample to 100 °C for 5 min and by the addition of 3.8  $\mu$ l of 200 mM phenylmethanesulfonyl fluoride. Digested samples were pelleted (13,000  $\times$  g, 10 min). 200- $\mu$ l aliquots of the supernatant were lyophilized and reconstituted in 50 or 100  $\mu$ l deionized water as required. The reconstituted plasma digest had a pH of 7.2 and contained 16  $\mu$ l of initial plasma volume.

**Desalting and Concentrating Digested Plasma Peptides for MALDI-TOF-MS**— $\mu$ C18 ZipTip pipette tips (Millipore, Schwalbach, Germany) were used according to the manufacturer's instructions to bind and desalt peptides from the plasma digest.

**In-solution Immunocomplex Formation and Purification Using Density Gradient Ultracentrifugation**—Each of the reconstituted plasma digest samples (50  $\mu$ l) was incubated for 1 h at room temperature with 10  $\mu$ g of one of the respective antibodies. Incubated samples were either processed by protein G magnetic bead enrichment as described below (controls) or as follows. A three-layer sucrose density

gradient was prepared by carefully pipetting the sucrose solutions into a 1.5 ml centrifugation tube (Beckman Coulter, Brea, CA) (bottom layer, 350  $\mu$ l of 30% sucrose, PBS; middle layer, 350  $\mu$ l of 20% sucrose, PBS; and top layer, 450  $\mu$ l of 10% sucrose, PBS). The sample (50  $\mu$ l) was carefully loaded onto the top of the sucrose gradient, and the sample tubes were placed into a TL-100 ultracentrifuge (Beckman Coulter) with fixed angle rotor (TLA-55). Centrifugation was carried out at 4 °C, 55,000 rpm (135,000  $\times$  *g* average relative centrifugal force) for 15 h. After centrifugation, the tubes were punctured at the bottom with a 20-gauge needle and fractions with defined volumes (50 or 500/400/300  $\mu$ l) removed using a pipette.

**Bead-based Model Assay**—Three bead-based immunoassays (Luminex Corp., Austin, TX) comprising biotinylated HA peptide (Biotin-Doa-Doa-YPYDVPDYA-NH<sub>2</sub>; Intavis) and rat anti-HA tag antibody (clone 3F10; provided by Elisabeth Kremmer, Munich, Germany) were established to compare and quantify the peptide-antibody complex, total peptide, and total antibody (C) in the controls and fractions obtained from ultracentrifugation: (a) Antibody and antibody-peptide complex were captured in a 1 h incubation with donkey anti-rat antibody-coupled beads (1000 beads/sample). After three washing steps, only the captured antibody-peptide complex was detected using streptavidin-PE conjugate (2.5  $\mu$ g/ml; Jackson ImmunoResearch). (b) Free peptides and antibody-peptide complexes were captured by a 1 h incubation with streptavidin-coated beads (1000 beads/sample). After washing, the captured peptides were detected by a 1 h incubation with 30  $\mu$ l of rat anti-HA antibody (1  $\mu$ g/ml), followed by washing and 45 min of incubation with 30  $\mu$ l of PE-labeled anti-rat detection antibody (2.5  $\mu$ g/ml; Jackson ImmunoResearch). (c) The total amount of antibodies was measured by a sandwich immunoassay starting with a 1 h incubation with donkey anti-rat antibody-coupled beads (1000 beads/sample). After washing, the captured antibodies were detected by 45 min of incubation with 30  $\mu$ l of PE-labeled anti-rat detection antibody (2.5  $\mu$ g/ml; Jackson ImmunoResearch). Covalent coupling of streptavidin (Pierce) and donkey anti-rat antibodies (Jackson ImmunoResearch) to carboxylated fluorescent beads (Luminex Corp.) was done using standard 1-ethyl-3-[3-dimethylaminopropyl]carbodiimide hydrochloride/*N*-hydroxysulfosuccinimide chemistry as previously described (32). All of the incubation steps were performed in MultiScreen 96-well filter plates (Millipore, Billerica, MA) at room temperature in an orbital shaker at 650 rpm. Blocking reagent for ELISA (Roche), 0.05% Tween 20 was employed as assay and dilution buffer in all steps. The median bead type-specific fluorescence was determined with a Luminex 100 IS system by measuring 100 bead events.

**Magnetic Bead-based Immunoaffinity Peptide Enrichment**—Reconstituted plasma digest samples (50 or 100  $\mu$ l) or fractions obtained after ultracentrifugation (500, 400, or 300  $\mu$ l) were incubated for 1 h at room temperature with 10  $\mu$ g of the respective antibodies. Antibody-peptide complexes were captured from samples with 5  $\mu$ l of protein G Dynabeads (Invitrogen) per  $\mu$ g antibody, washed, and eluted in a magnetic particle handling system (KingFisher) as described previously (19, 24, 33). 1  $\mu$ l of 50  $\mu$ l of eluted peptide solution representing 320 nl of plasma was spotted onto a prespotted  $\alpha$ -cyano-4-hydroxycinnamic acid AnchorChip (Bruker Daltonics, Bremen, Germany) for mass spectrometric analysis.

**Quantification of Vitamin K-dependent Protein S**—Recovery and concentration of the endogenous plasma vitamin K-dependent protein S peptide were determined using isotopically labeled NIPGDFF-CECEGYR<sup>1</sup> peptide (molecular weight, 1851.73) that was spiked into digested plasma samples or PBS, 0.3% *n*-octyl- $\beta$ -D-glucopyranoside before incubation with antibodies to give different concentrations in 100  $\mu$ l of volume. In addition, a blank sample without labeled peptide was run in each assay. Assay sensitivity was determined by the analysis of signal to noise values (minimum 3) for this peptide. En-

dogenous protein S peptide (*m/z* 1842.72) amount was analyzed by comparing the signal to noise values for *m/z* 1842.72 and 1852.73). To determine endogenous peptide recovery, different concentrations of isotopically labeled NIPGDFF-CECEGYR<sup>1</sup> peptide were spiked into the immunoprecipitated blank sample just before spotting onto the MALDI target, and endogenous peptide amounts were compared for peptide spike-in before and after ultracentrifugation/immunoprecipitation. Four independent experiments were performed. Each sample was spotted four times onto the MALDI target, and the mean values were taken.

**Peptide Identification by MALDI-TOF-MS/MS**—MS and MS/MS spectra were obtained using an Ultraflex III MALDI-TOF/TOF mass spectrometer equipped with a LIFT unit for tandem MS analysis (Bruker Daltonics). Mass spectrometry was performed in positive ion reflectron mode with a deflector cutoff up to 550 Da. All of the spectra were analyzed using flexAnalysis 3.0 software (Bruker Daltonics). Mass calibration was carried out using the prespotted calibrants on the AnchorChip target plates. The flexAnalysis peptide mass fingerprint method was used for automatic annotation of ion masses and generation of peak lists in the mass range from 700 to 5000 Da. Only peaks with a signal to noise ratio higher than 10 were selected for MS/MS analysis. The laser power and number of shots (2000–4000) were adjusted manually by the operator. Monoisotopic masses of annotated peaks were compared with SwissProt database entries restricted to human taxonomy (release 2010\_07, containing 20,253 human sequence entries) using the ProteinScape 2.1 software (Bruker Daltonics) and the MASCOT 2.3 search engine (Matrix Science, London, UK). MASCOT searches were restricted to trypsin or semi-trypsin digestion with one partial cleavage. Carbamidomethylation of cysteine was set as a fixed modification. No variable modifications were taken into account. Mass tolerances were set to 50 ppm for precursor ions and 0.7 Da for fragment ions. Only peptides that were identified by Mascot ion scores that indicated identity or extensive homology with *p* < 0.05 were regarded as valid. Annotated MSMS spectra of all peptide identifications can be found in [supplemental Fig. 3](#). The data associated with this manuscript may be downloaded from ProteomeCommons.org Tranche using the following hash code: T1p0LTzWUobLpZrN+ely4CWICuV6Hty6vxhd0Sd0i/SXAoTm3e6HkHFMsFA2MtOSnzwXTdWURbWP9eYLiUBafMVCe0AAAAAAAbOEg = =.

**Statistical Analysis**—Nonparametric group comparisons were performed using the Mann-Whitney test. For multiple group comparisons, the nonparametric Kruskal-Wallis test was used. All of the statistical analysis was carried out using Statistix version 1.8 (Statistix, Nedlands, Australia).

## RESULTS

**Antigen Selection and Antibody Characterization**—Mass spectrometry-based triple X proteomics employs antibodies capable of recognizing groups of tryptic peptides containing common short terminal epitopes. To assess the suitability of the TXP approach for plasma proteomics, antibodies were generated against 15 different antigens. The selection was based on two criteria. First, the antibodies were required to bind to N- or C-terminal epitopes of tryptic peptides from plasma proteins. Second, the panel of antibodies was required to target peptides present at a broad range of concentrations (mg/ml to pg/ml; Table I). This was done to obtain an estimation of the dynamic range of the assay. After antibody generation the antibodies were purified by peptide affinity chromatography. The binding affinity of the purified IgGs was evaluated using a competitive immunoassay setup (29, 34).

TABLE I  
TXP epitopes and target peptides of the 15 TXP antibodies used

Antibody specificity	Specified target peptide	Sequence	Plasma level, $\mu\text{g/ml}$	Reference	
VLLD	N-terminal	Complement C3	VLLDGVQNP	1300	38
		Apolipoprotein B-100	VLLDQLGTTISFER	915	39
VELED	N-terminal	Fibrinogen $\gamma$ chain	VELEDWNGR	915	39
		Fibrinogen $\alpha$ chain	VELEDWAGNEAYAEYHFR	1250	39
AFVK	C-terminal	Apolipoprotein B-100	DAVEKQPQFTIVAFVK	915	39
		Serotransferrin	DGAGDVAFVK	4000	38
DAPK	C-terminal	Ceruloplasmin	IYHSHIDAPK	280	38
DTWK	C-terminal	Alkaline phosphatase	LDGLDLVDTWK	0.04	38
DYGK	C-terminal	Apolipoprotein A-II	EPCVESLVSQYFQTVTDYGK	244	38
EGYR	C-terminal	Vitamin K-dependent protein S	NIPGDFECECEPEGYR	25	39
EHLR	C-terminal	Receptor tyrosine-protein kinase erbB-2	VCYGLGMEHLR	0.01	38
ESFR	C-terminal	Tenascin	APTAQVESFR	1	38
EVL	C-terminal	Serum paraoxonase/arylesterase 1	IFFYDSENPPASEVLR	59.3	38
FPPK	C-terminal	Tumor necrosis factor receptor superfamily member 11B	WTTQETFPPK	0.000035	38
LEVK	C-terminal	Keratin, type I cytoskeletal 19	ALEAANGELEVK	0.0024	38
PIEK	C-terminal	Leptin receptor	YYIHDHFIPIEK	0.0048	38
QGYR	C-terminal	Vitamin K-dependent protein Z	TDGCQHFCLPGQESYTCSCAQGYR	3	39
VEVSR	C-terminal	Serum albumin	VPQVSTPTLVEVSR	41000	38
		Clusterin	LFDSDPITVTVPVEVSR	100	39

Here, the antibodies were incubated in solution with different amounts of soluble peptide antigen, and the half-maximal effective concentration of the peptide capable of inhibiting the antibody-antigen interaction with peptides immobilized on a solid-surface was determined. This method was chosen because polyclonal antibody preparations consist of different antibody populations showing different dissociation constants ( $K_D$ ). Therefore a true  $K_D$  cannot be determined for polyclonal antibodies (30). Nevertheless, the  $EC_{50}$  measurement can provide a good measure of affinity to compare polyclonal antibodies. The results are given in [supplemental Table 1](#) showing  $EC_{50}$  in the nanomolar range suitable for immunoprecipitation procedures.

**Immunoaffinity Enrichment of Plasma Digest Peptides with TXP Anti-EGYR Antibodies**—As a proof-of-principle, we investigated whether TXP antibodies targeting the short C-terminal sequence EGYR were capable of enriching peptides from a tryptic digest of human blood plasma. Anti-EGYR antibodies were chosen as EGYR-containing tryptic peptides were common products of moderately abundant ( $\mu\text{g/ml}$ ) human plasma proteins as determined by *in silico* digestion. Anti-EGYR antibodies were incubated with the digested sample, and antibody-peptide complexes were isolated using magnetic protein G beads. The captured peptide pool was eluted and analyzed by MALDI-TOF/TOF MS. Fig. 1A shows a representative spectrum obtained following immunoprecipitation with anti-EGYR antibodies. All of the peaks with a signal to noise ratio higher than 10 were subject to post source decay fragmentation and comparison with the Mascot database. The search identified two peptides (VVCSCTEGYR and NIPGDFECECEPEGYR) containing the C-terminal EGYR

epitope assignable to coagulation factor IX and vitamin K-dependent protein S, respectively (Table II). Several other peptides derived from albumin or other highly abundant proteins were also identified ([supplemental Table 2](#)). In contrast, C18 reverse phase purification of the plasma digest without immunoaffinity enrichment only yielded nontargeted peptides derived from highly abundant proteins (Fig. 1B). These data suggested that although the TXP assay had been effective in isolating two proteins of interest, the nonspecific binding of peptides derived from high abundant plasma proteins had potentially hampered the detection of other relevant target proteins.

To identify the factors responsible for the presence of the nontargeted peptides, two control assays were carried out. In the first assay the same procedure described above was employed but without the TXP antibodies. The resulting mass spectrum revealed several peptides, most of which were shown to be derived from albumin upon fragmentation and database searching (Fig. 1C and [supplemental Table 2](#)). None of the peptides containing the C-terminal EGYR sequence were detected here. In a second control experiment, the assay was repeated with the omission of the magnetic protein G-coupled beads as well as the antibodies. Remarkably, the nonspecific albumin peptides were still clearly visible in the mass spectra, albeit at a 5–10-fold lower intensity (Fig. 1, C and D). This suggests that even the disposable plastic components of the magnetic bead handler contributed to the presence of the contaminating peptides. Based on these findings, we set about developing an in-solution purification step capable of separating the antibody-peptide complexes from the nonspecifically bound peptides present in the digested

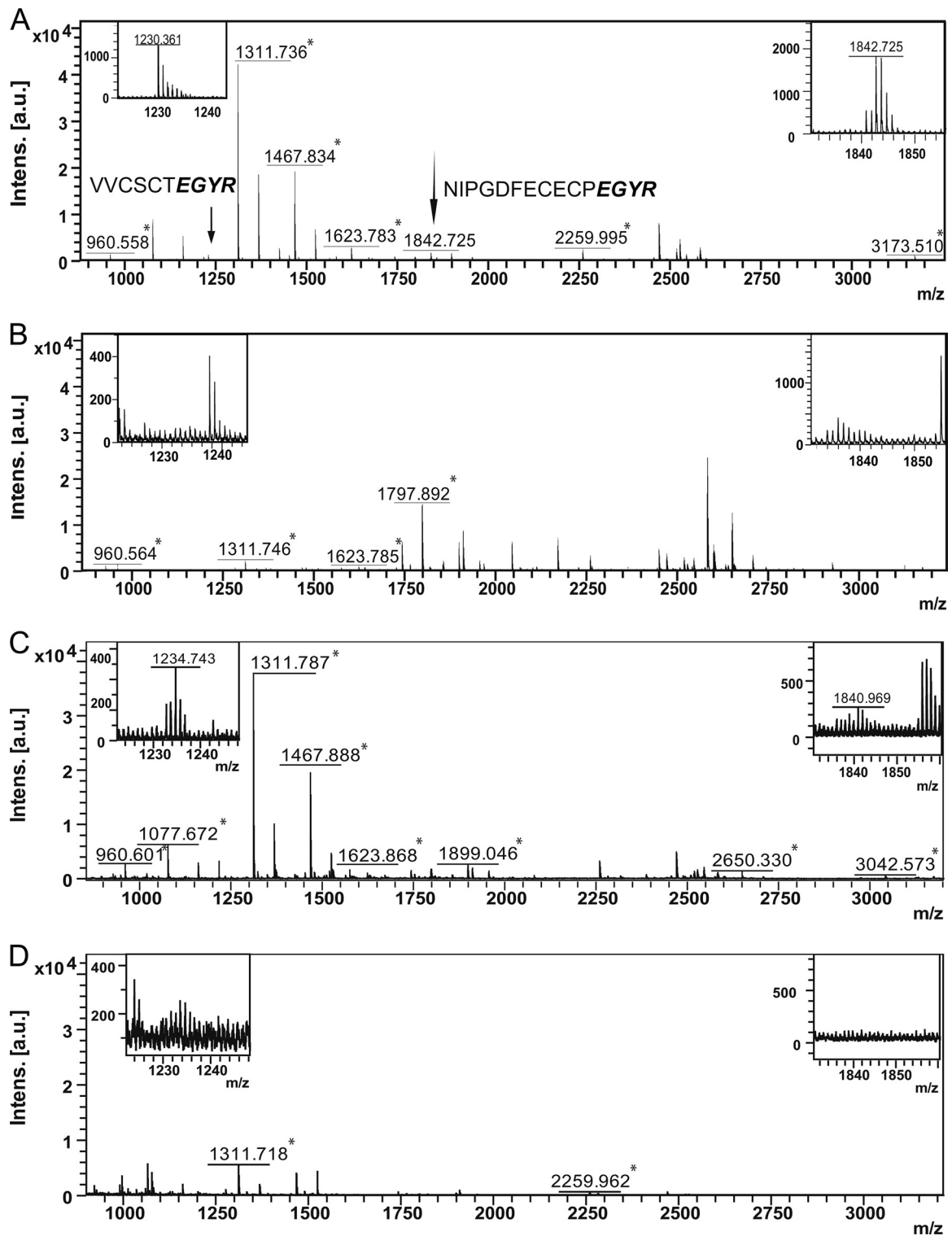


FIG. 1. Mass spectra of tryptic digested human plasma after anti-EGYR TXP immunoaffinity enrichment (A), after  $\mu$ ZipTip C18 peptide enrichment without immunoaffinity enrichment (B), after the antibody incubation step was omitted from the immunoaffinity enrichment step (C), and after the antibody incubation step and the incubation with the protein G beads were omitted (D). Tryptic peptides derived from highly abundant human albumin are marked with asterisks.

TABLE II  
Comparison of identified peptides harboring the C-terminal EGYR target sequence

Peptide identification was performed using Mascot search algorithms with peptide fragment mass spectra generated by MALDI-TOF/TOF analyses.

Protein name	Amino acid sequence	<i>m/z</i>	Reported human plasma level	Peak detected without/with ultracentrifugation
Coagulation factor IX	VVCSCTEGYR	1230.49	4 $\mu\text{g/ml}$ (Ref. 48)	+/+
Isoform 2 of filamin-A	MDCQECPEGYR	1444.48	35 ng/ml (Ref. 35)	-/+
Vitamin K-dependent protein S	NIPGDFECECPEGYR	1842.68	25 $\mu\text{g/ml}$ (Ref. 39)	+/+

plasma sample. We chose to explore the use of ultracentrifugation, so as to minimize contact with surfaces to which the contaminating peptides could adhere.

**Bead-based Immunoassays for the Quantification of HA Peptide, Anti-HA Antibody, and Anti-HA Antibody/HA-Peptide Complexes**—Three bead-based sandwich immunoassays incorporating synthetic biotinylated HA peptide and anti-HA tag antibody were established to quantify the distribution of peptide, antibody, and antibody-peptide complex after ultracentrifugation. In the first assay, antibody-peptide complexes were captured using donkey anti-rat antibody-coated beads and detected with a streptavidin-PE conjugate. In the second assay, the biotinylated HA peptide was captured with streptavidin-coupled beads, incubated with rat anti-HA antibodies, and detected with donkey anti-rat antibody-PE conjugate. In the third assay, the total amount of antibody was quantified in a sandwich immunoassay format using two anti-rat specific antibodies as capture and detection molecules. Incorporating the high affinity HA antibody and streptavidin capture molecules enabled highly sensitive detection. Working ranges of the assays were from 0.08 to 2 ng/ml and 0.008 to 0.7  $\mu\text{g/ml}$  for the peptide and antibodies, respectively (supplemental Fig. 1). The immunocomplex could only be relatively quantified.

**Density Gradient Ultracentrifugation for the Purification of Antibody-Peptide Complexes from Plasma Digests**—A mixture containing a 250-fold excess of HA-peptide (250  $\mu\text{g}$ ) to anti-HA antibody was pipetted onto the top of the sucrose density gradient. This antibody to peptide ratio was chosen because it resembles a typical molar excess of tryptic fragments derived from high abundant plasma proteins to antibody in an immunoaffinity setup. After ultracentrifugation, 27 fractions were collected as described under “Experimental Procedures.” The samples were subsequently diluted, and the amounts of peptide and antibody were quantified relative to an external standard using the assays described above. The analyses showed that the antibodies and antibody-peptide complexes were present in the lower fractions of the gradient (Fig. 2A, fractions 1–15), whereas free HA-peptide was mainly found in the upper fractions (Fig. 2A, fractions 10–27). 70% of the antibody (both free and peptide-bound) and less than 1% of excess peptide were present in the lower 500  $\mu\text{l}$  of the sucrose gradient (Fig. 2B).

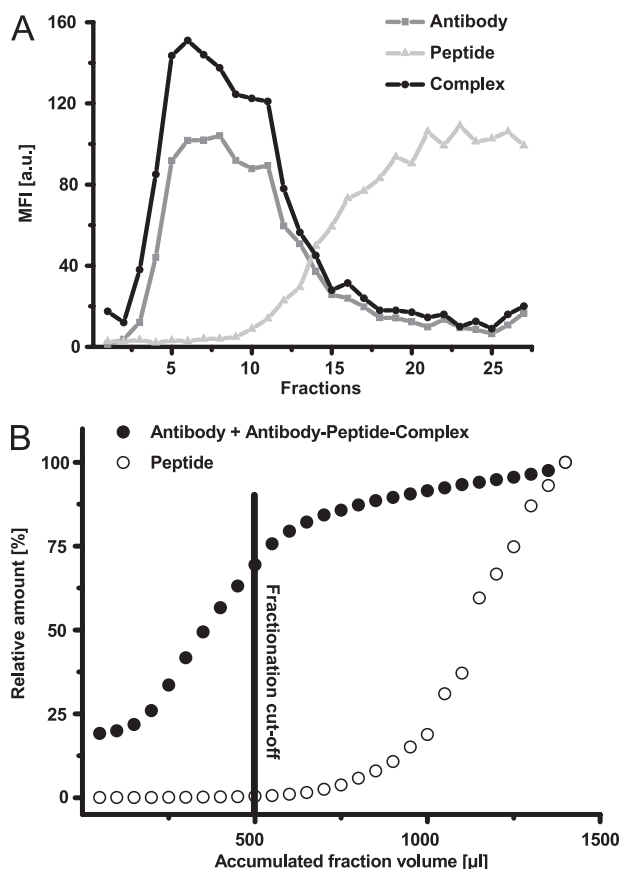


FIG. 2. Distribution of free monoclonal rat anti-HA antibody, biotinylated HA peptide, and the resulting antibody-peptide complex following 15 h of sucrose gradient ultracentrifugation. 27 fractions (50  $\mu\text{l}$  each) were collected and analyzed using the Luminex™ immunoassay platform. A, mean fluorescence intensity (MFI) values of each analyte are plotted per fraction (ascending numbers from bottom to top of sample tube). For clarity, mean fluorescence intensity values divided by 10 are reported for the antibody-peptide immunocomplex, and mean fluorescence intensity was divided by 100 for the peptide. B, the fraction of the total amount of anti-HA antibody and biotinylated HA peptide accumulated with total collected fraction volume measured from the bottom of the sample tube. The fractionation cutoff represents the volume containing 70% accumulation of peptide-antibody immunocomplex but less than 0.5% of the residual free peptide. a.u., arbitrary units.

**Immunoaffinity Enrichment of EGYR-containing Peptides Using Density Gradient Purification and Magnetic Bead Separation**—Purification of antibody-peptide complexes from

plasma by density gradient ultracentrifugation was evaluated using anti-EGYR antibodies. The ultracentrifugation step was inserted between the incubation of the plasma digest with the anti-EGYR antibodies and precipitation using protein G magnetic beads. Three fractions of 500  $\mu\text{l}$  (containing 70% of the peptide-antibody complex; see Fig. 2), 400  $\mu\text{l}$ , and 300  $\mu\text{l}$  were collected from the bottom of the centrifugation tube, respectively. For process control purposes, antibody sedimentation was visually verified using Cy5-labeled IgG (Fig. 3, B–D, insets). The MS spectrum of the top gradient fraction (Fig. 3B) was very similar to that of the control where no centrifugation step was implemented (Fig. 3A), predominantly comprising peptides derived from the highly abundant proteins, such as  $m/z$  1160.591, 1311.744, or 1467.843. In contrast, the two target peptides ( $m/z$  1230.534 and 1842.747) corresponding to coagulation factor IX and vitamin K-dependent protein S were clearly detectable in the bottom fraction (Fig. 3D). They were also detectable in the middle fraction (Fig. 3C) along with the high abundant peptides, albeit marginally. Interestingly, a previously undetected peptide (MDCQECPEGYR) derived from the protein filamin-A could also be identified in the peptide complex-purified fraction (Fig. 3D).

To obtain some measure of the improved sensitivity gained through the implementation of the ultracentrifugation procedure, the signal to noise value of the NIPGDFECECEGYR target peptide ( $m/z$  1842.747, vitamin K-dependent protein S) was compared with the signal to noise values of  $\alpha$ -1-acid glycoprotein 1 ( $m/z$  1160.70, WFYIASAFR) and human serum albumin ( $m/z$  1311.77, HPDYSVLLLLR; and  $m/z$  1467.85, RHPDYSVLLLLR). Ultracentrifugation improved the signal to noise ratio of the EGYR target to nonspecific peptides more than 2000 fold (Fig. 4A).

Quantitative assessments of the ultracentrifugation procedure were performed using isotopically labeled NIPGDFECECEGYR<sup>+</sup> peptides. Different concentrations of labeled peptides were spiked into plasma digest samples before incubation with the antibodies. The comparison of the results obtained with and without ultracentrifugation revealed a drastically increased signal to noise ratio for peaks derived from the isotopically labeled peptide after ultracentrifugation (Fig. 4B). For all concentrations tested, at least a 25-fold increase in signal to noise ratio was observed with the use of ultracentrifugation in comparison with the procedure without ultracentrifugation. Robust signals with signal to noise ratios of  $>10$  were obtained without ultracentrifugation for 17.1 nM of spiked-in peptide, whereas a 10-fold lower concentration could still be detected with ultracentrifugation. A peptide concentration of  $\sim 45$  nM had to be applied without ultracentrifugation to result in the same signal to noise ratios as with 3 nM using ultracentrifugation. Thus, a 25-fold sensitivity improvement could be achieved by the use of ultracentrifugation.

In addition, we determined the peptide recovery after ultracentrifugation and immunoprecipitation on the basis of vitamin K-dependent protein S peptide. This was achieved by

spiking the isotopically labeled peptide into the plasma digest before incubation with the antibodies and into the immunoprecipitate of a different aliquot of the same digest sample just before spotting onto the MALDI target. The recovery of endogenous peptide was determined as  $51 \pm 13\%$ . Furthermore, the endogenous protein concentration was determined as  $24.2 \pm 3.7 \mu\text{g/ml}$ .

*Combined Ultracentrifugation and TXP Immunoaffinity Assay Using 15 TXP Antibodies*—Based on the encouraging results described above, we investigated the impact of the ultracentrifugation purification step using a panel of MS-based TXP immunoaffinity assays targeting a broad range of tryptically digested plasma proteins. In total, 42 plasma peptides were identified requiring only 15 TXP antibodies (Table III). A maximum of three peptides sharing the same C-terminal TXP tag sequence were detectable by one single antibody (epitope EGYR). Peptides were also detected where one amino acid did not correspond to the TXP tag sequence. Nevertheless, the cross-reactions can be explained by similar physicochemical properties of the respective amino acid. This broader capture capacity enabled the detection of up to six different peptides by one TXP antibody (epitope ESFR) leading to the successful identification of five different plasma proteins. In the majority of cases, at least two peptides could be identified per antibody. Exceptions were the anti-DAPK and anti-LEVK antibodies where only one peptide could be identified for each. For four of the antibodies (epitopes DTWK, ESFR, LEVK and QGYR) only peptides with one amino acid mismatch in their terminal sequence could be identified.

The incorporation of the density gradient purification step permitted the identification of 37 peptides from at least one of three technical replicate experiments. 57% of these were identified in all three replicates. Notably, 13 peptides were uniquely identified with the procedure incorporating ultracentrifugation. In comparison, only 29 peptides were identified without the added purification step. Of these, 55% could be identified in all three replicates. Five peptides were identified solely in the noncentrifuged controls.

To evaluate any benefits in the sensitivity afforded by the added purification step, a comparison of the signal to noise ratios for one target peptide was compared with that of three nonspecific high abundant peptides. For 10 of 15 TXP antibodies investigated, a significantly improved signal to noise ratio was observed for the target peptide where the centrifugation step had been implemented (Fig. 4 and [supplemental Fig. 2](#)).

## DISCUSSION

The vast library of organo-specific, disease-diagnostic information contained within blood plasma, combined with its availability and ease of sampling, make it the most significant clinical sample for biomarker discovery to date. However, accessing this information is a major challenge given the complexity and concentration range of its protein composi-

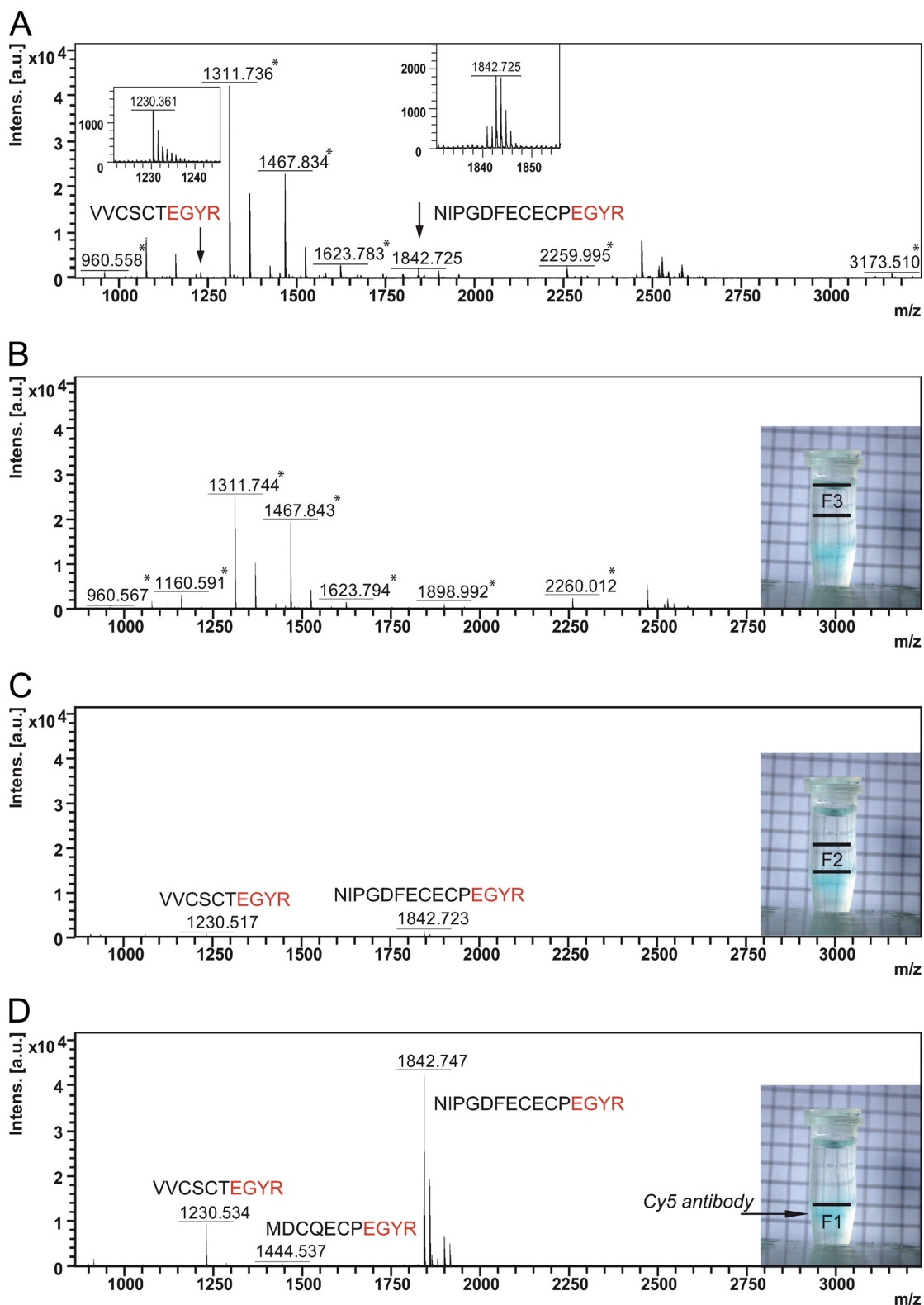
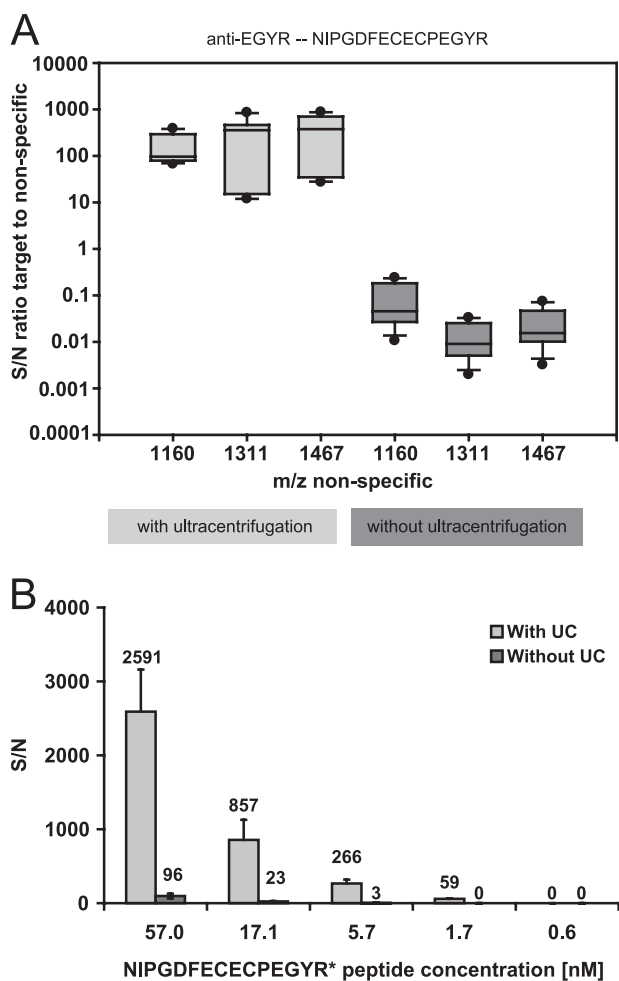


FIG. 3. Mass spectra of tryptic plasma peptides enriched using the anti-EGYR TXP antibodies without sucrose density gradient separation (A), in the top 300- $\mu$ l fraction (B), in the middle 400- $\mu$ l fraction (C), and in the bottom 500- $\mu$ l fraction following sucrose density gradient ultracentrifugation (D). The samples containing antibodies conjugated with the dye Cy5 were added to each ultracentrifuge run to visualize the location of antibodies within the sucrose layers after centrifugation (*insets*). The peptides corresponding to nontargeted high abundant plasma proteins are marked with asterisks. *a.u.*, arbitrary units.





**FIG. 4. Impact of ultracentrifugation step on peptide quantification.** *A*, distribution of signal to noise ratios for target peptide NIPGDFECECEPEGYR ( $m/z$  1842.68, vitamin K-dependent protein S) relative to three nonantibody targeted peptides from two different proteins  $\alpha$ 1-acid glycoprotein 1 ( $m/z$  1160.70, WFYIASAFR) and two peptides from human serum albumin ( $m/z$  1311.77, HPDYSVLLLLR; and  $m/z$  1467.85, RHPDYSVLLLLR) comparing the assay with and without the ultracentrifugation step. The data from three assay replicates are included in one box plot. The signal to noise (S/N) ratios of the values generated with the ultracentrifugation procedure are significantly higher compared with the respective values of the assays without ultracentrifugation ( $p < 0.001$ ). *B*, MALDI signal to noise values for different spike-in concentrations of isotopically labeled NIPGDFECECEPEGYR\* peptide ( $m/z$  1852.73) in TXP assays with plasma digest including and excluding ultracentrifugation. The concentrations refer to 100  $\mu$ l of reconstituted plasma digest, which are derived from 16  $\mu$ l of plasma. A representative experiment is shown. The error bars represent the standard deviation of four different MALDI spots of the same sample.

tion. In this study, the suitability of a MALDI mass spectrometry-based group-specific immunoaffinity enrichment assay for the identification of human blood plasma proteins was investigated. As previously reported, groups of peptides sharing a common N- or C-terminal 4–5-amino acid motif can be enriched from tryptically digested biological samples using

so-called TXP antibodies generated against these short terminal epitopes (24). Although the TXP approach for the identification of plasma peptides was successful, the mass spectra produced were dominated by peaks corresponding to nonspecific high abundant plasma peptides. The detrimental effects of these peptides upon the detection of the targeted low abundance peptides is well documented (35). Sucrose density gradient ultracentrifugation following incubation of the tryptic plasma digest with an antibody led to the removal of 99% of peptides not bound to antibodies. The application of a panel of TXP antibodies generated against 15 different C- or N-terminal sequences to a plasma protein digest using a led to the successful identification of 37 peptides, of which up to six were identified using just one antibody. Our findings support the combined application of MALDI MS-based TXP immunoaffinity assays and density gradient purification for the identification of multiple plasma proteins. To our knowledge, this is the first study that uses immunoaffinity-MALDI MS without LC separation for the targeted and nontargeted identification of several plasma proteins.

Peptide targeting immunoaffinity assays described by us and others (24, 36) comprise incubation of digested plasma with antibodies followed by solid phase precipitation using protein G-coated magnetic beads, elution of the targeted peptides, MALDI-TOF/TOF MSMS analysis, and subsequent protein assignment by database comparison. We successfully isolated two tryptic plasma peptides using a TXP antibody specific for the short C-terminal EGYR sequence originating from coagulation factor IX and vitamin K-dependent protein S. The detection of these two proteins, which have been reported to be present at 4 and 25  $\mu$ g/ml in plasma, was not possible when only using C18 reversed phase ZipTip columns. This was to be expected, however, given the concentration range and breadth of the plasma proteome and the matrix and analyte ion suppression effects characteristic of the MALDI (along with the electrospray) ionization techniques (35, 37). Nevertheless, the domination of nontargeted peptides derived from highly abundant proteins following anti-EGYR antibody immunoprecipitation was unexpected. Control experiments revealed that their presence could be mainly traced back to their nonspecific binding to the large surface of the protein G beads (Fig. 1C), a problem also reported by other groups (20, 25).

As a result of these findings, we began searching for a solid phase-free separation technique. Classical density gradient ultracentrifugation was particularly attractive because it enables the separation of antibody-complexed peptides while minimizing exposure of the dominant high abundant protein derived peptides to large surface areas where nonspecific binding can occur. The separation of protein-antibody complexes from free proteins in solution has previously been reported (27, 28). Using a model system consisting of biotinylated HA peptide and anti-HA tag antibody and employing various bead-based sandwich immunoassays, we were

TABLE III  
List of peptides identified from the immunofluorescence enrichment of plasma peptides using the 15 TXP antibodies  
The TXP epitopes either C- or N-terminal are given in the first column. TXP epitopes are shown with bold letters. NK, not known.

TXP tag	Molecular mass, Da	Sequence	Protein name	Accession number	Plasma concentration, µg/ml	Reference	Ultracentrifugation			No ultracentrifugation		
							Mascot score	Identified	Identified in triplicate	Mascot score	Identified	Identified in triplicate
VLLD	1110.57	<b>VLLD</b> GVQMPR	Complement C3	P01024	1.3E+03	38	63	X	X	71	X	X
VLLD	1591.86	<b>VLLD</b> QLGTTLSFER	Apolipoprotein B-100	P04114	9.15E+02	39	85	X	X	59	X	X
VLLD	1702.79	VFLDCNYITIELR	Complement C3	P01024	1.3E+03	38				57	X	X
VELED	1117.53	<b>VELED</b> WNGR	Isoform γB of fibrinogen γ chain	P02679	9.15E+02	39	64	X	X	64	X	X
VELED	2198.95	<b>VELED</b> MAGNEAYAEYHFR	Isoform 1 of Fibrinogen α chain	P02671	1.25E+03	39	80	X	X	55	X	X
AFVK	978.47	DGAGDVA <b>AFVK</b>	Serotransferrin	P02787	4.00E+03	38	30	X	X	30	X	X
AFVK	1152.58	QPSAFA <b>AFVK</b>	Complement C3	P01024	1.3E+03	38	45	X	X	66	X	X
DAPK	1180.61	IYHSHID <b>APK</b>	Ceruloplasmin	P00450	2.80E+02	38	67	X	X	38	X	X
DTWK	1601.84	YSALLTPAEGTGWK	Apolipoprotein B-100	P04114	9.15E+02	39	59	X	X			
DTWK	1893.89	ASTFNGYDNGIHWATWK	Isoform γB of Fibrinogen γ chain	P02679	9.15E+02	39	95	X	X			
DYGG	1074.54	LDELRDGK	Serum albumin	P02768	4.10E+04	38				35	X	X
DYGG	2350.13	EPCVESLVSQFQTV <b>TDYGG</b>	Apolipoprotein A-II	P02652	2.44E+02	38	141	X	X	170	X	X
EGYR	1230.49	VVCSCT <b>EGYR</b>	Coagulation factor IX	P00740	4.50E+00	48	66	X	X			
EGYR	1444.51	MDCQCE <b>EGYR</b>	Isoform 2 of fibrin-A	P21333	3.50E-02	40	35	X	X	62	X	X
EGYR	1842.68	NIPGDFECFC <b>EGYR</b>	Vitamin K-dependent protein S	P07225	2.50E+01	39	113	X	X	54	X	X
EHLR	1395.78	SSNLLILEEHLK	Complement factor H	P08603	5.00E+02	39	48	X	X			
EHLR	1545.69	GFMQTYDDHLR	Apolipoprotein C-IV	P55056	1.00E+00	39	38	X	X			
EHLR	2509.05	SCVGETESTQCEDE <b>EHLR</b>	Complement component C7	P10643	5.20E+01	38	163	X	X	136	X	X
ESFR	1126.55	LHVDPENFR	Hemoglobin subunit δ	P68871	3.25E+01	39	56	X	X	78	X	X
ESFR	1169.51	SSALDMENFR	Inter-α-trypsin inhibitor heavy chain H2	P19823	2.10E+02	39	32	X	X	42	X	X
ESFR	1519.72	ALYLQYD <b>ESFR</b>	Ceruloplasmin	P00450	2.80E+02	38	108	X	X	98	X	X
ESFR	1647.82	KALYLQYD <b>ESFR</b>	Ceruloplasmin	P00450	2.80E+02	38	59	X	X	70	X	X
ESFR	1927.92	SLAELGHLQ <b>QVEEFR</b>	Apolipoprotein A-IV	P06727	1.90E+02	39	52	X	X	80	X	X
ESFR	2707.10	HOQEFPTYYEPTNDEICEA <b>FR</b>	Vitamin D-binding protein	P02774	5.50E+02	39	128	X	X	148	X	X
EVL	774.42	ECEELLR	Sterile α and TIR motif-containing protein 1	Q6SZW1	NK	-	31	X	X			
EVL	1290.70	SLTINIMEILR	Fibrinogen α chain	P02671	1.25E+03	39	72	X	X			
EVL	1629.81	SLTINIMEILR	Fibrinogen α chain	P02671	1.25E+03	39	139	X	X	51	X	X
EVL	1883.90	IFFYDSENPFA <b>SEVLR</b>	Serum paraoxonase/arylesterase	P27169	5.93E+01	38	145	X	X	42	X	X
EVL	2199.10	YNPVVIDFEMOPI <b>HEVLR</b>	Complement component C8 α chain	P07357	4.70E+01	39	68	X	X			
FPPK	1492.65	TFSCGDICN <b>FPPK</b>	C4b-binding protein α chain	P04003	3.65E+02	39	70	X	X			
FPPK	2619.28	THTCPFCFAPPELLGGPSVFL <b>FPPK</b>	Anti-RhD monoclonal T125 γ1 heavy chain precursor	P01857	4.30E+03	39	116	X	X			
LEVK	1419.72	VQFELHQ <b>VEVK</b>	Inter-α-trypsin inhibitor heavy chain H2	P19823	2.10E+02	39	50	X	X	75	X	X
PIEK	824.48	GLPAP <b>PIEK</b>	Ig γ-2 chain C region	P01859	2.84E+03	39	55	X	X	53	X	X
PIEK	838.49	ALPAP <b>PIEK</b>	Ig γ-1 chain C region	P01857	4.30E+03	39	66	X	X	64	X	X
PIEK	1266.74	VSNKALPAP <b>PIEK</b>	Ig γ-1 chain C region	P01857	4.30E+03	39	36	X	X	36	X	X
QGYR	1022.55	ATVVYQGER	β2-Glycoprotein 1	P02749	2.25E+02	39	39	X	X	47	X	X
QGYR	1110.54	STTPDITGYR	Fibronectin	P02751	3.00E+02	39	32	X	X	32	X	X
QGYR	1330.74	LNMGITDLOGLR	Complement C4-A	P0C0L4	1.00E+02	39	40	X	X	40	X	X
QGYR	1712.79	GECQAEVLF <b>QGYR</b>	Hemopexin	P02790	8.25E+02	39	88	X	X	89	X	X
VEVSR	1511.86	VPOQVSTPTLV <b>VEVSR</b>	Serum albumin	P02768	4.10E+04	38	127	X	X	112	X	X
VEVSR	1639.95	KVPQVSTPTLV <b>VEVSR</b>	Serum albumin	P02768	4.10E+04	38	125	X	X			
VEVSR	1873.99	LFDSDPITVTPV <b>VEVSR</b>	Clusterin	P10909	1.0E+02	39	25	X	X			

able to quantitatively demonstrate the efficient separation of peptide-antibody immunocomplexes from excess peptides (Fig. 2).

The centrifugation purification step was subsequently tested using a TXP immunoprecipitation assay targeting tryptic plasma peptides containing the C-terminal EGYR sequence. After ultracentrifugation, the sucrose gradient was collected in three fractions (500, 400, and 300  $\mu$ l), which were then processed using protein G-coated magnetic beads. Analyses of the gradient fractions by MALDI mass spectrometry revealed a dramatic reduction in background signal arising from nontargeted high abundant peptides in the bottom 500- $\mu$ l fraction (Fig. 3D). In the case of the targeted vitamin K-dependent protein S-derived peptide, this resulted in an increased signal to noise ratio of over 2000 relative to the nonspecifically bound high abundant peptides (Fig. 4A). Moreover, removal of the unwanted peptides led to the detection of the peptide MDCQCEPEGYR derived from filamin-A. The enhanced sensitivity afforded by the workflow incorporating the centrifugation step was confirmed by a quantitative comparison using vitamin K-dependent protein S peptide. The signal to noise ratio of the ultracentrifugation assay for this specific peptide increased by factor 25 in average across a concentration ranging from 1.7 to 57 nM (Fig. 4B). In addition, 50% recovery was determined for the protein S peptide using the ultracentrifugation workflow. This fits well to the 70% antibody recovery in the bottom fraction after ultracentrifugation presented in Fig. 2. The estimated level of endogenous vitamin K-dependent protein S (24.2  $\mu$ g/ml) is in accordance with the values reported elsewhere (39).

We further compared the two procedures using 14 additional TXP antibodies for the analysis of a tryptic plasma digest. The workflow incorporating the ultracentrifugation step yielded 37 peptides *versus* 29 without (Table III). This can be explained by the improved signal to noise ratios of targeted to nonspecifically bound peptides, which was observed for most of the antibodies (supplemental Fig. 2). This resulted in an improvement of sensitivity and robustness of the assay shown by the increase from 16 to 21 peptide identifications in all three triplicates following ultracentrifugation purification (Table III).

On the whole, target peptides (Table I) from proteins with an abundance in plasma in the lower  $\mu$ g/ml range were identified (Table III). However, filamin-A, which is reported to be present at a concentration of 40 ng/ml (40), was also detected using just 16  $\mu$ l of plasma. This is within the range of current reports using peptide immunoprecipitation without protein depletion combined with multiple reaction monitoring techniques (41). They report detection limits in the lower ng/ml range or below from plasma volumes of 50  $\mu$ l or less (19, 20, 42). We were nevertheless surprised that our assay did not prove to be more sensitive following removal of nonspecific peptides. Maximum sensitivity of the assay was therefore tested by applying different amounts of peptide in PBS, 0.3% *n*-octyl-

$\beta$ -D-glucopyranoside instead of plasma digest. We showed that 600 amol of peptide in 100  $\mu$ l is sufficient for detection using the established approach (supplemental Fig. 3). This equates to 37.5 pM or 3 ng/ml of a plasma protein with a molecular weight of 75,000 Da. As such, the method is applicable for the detection of medium-abundant proteins. 10 amol of peptide was detected on spot, which is within the range of immuno-MALDI sensitivity (43). The discrepancy in observed sensitivity depending on the assay matrix, however, might be explained by the limitations of the mass spectrometry method employed. Using MALDI-TOF mass spectrometry, a dynamic range of only 2–3 orders of magnitude can be covered with one ionization event as a result of the limited range of the multichannel plate detector and the limited analyte to matrix ratio required for successful ion generation. In the experiments presented here, tryptic peptides derived from proteins covering concentrations that differed by a factor of between 200 and 1000 were detected with one single antibody. This is well in line with the reported dynamic detection range of MALDI mass spectrometry. Because TXP antibodies in this study typically capture at least one peptide present in the higher  $\mu$ g/ml range, assay sensitivities below ng/ml are probably unachievable using MALDI MS. The use of more selective mass spectrometry methods such as MALDI multireaction monitoring may increase the dynamic range of the measurable analytes (44). Additionally, TXP antibodies specifically targeting lower abundant analytes may also increase the overall sensitivity of the assay.

To evaluate our assay and contrast it with those of others working in the field, we compiled lists of tryptic peptides that should have been detected by the incorporated TXP antibodies according to two empirical plasma proteome databases, Peptide Atlas Plasma (build May 2010 containing 16,987 entries (45)) and the database created by the HUPO Plasma Proteome Project (46) (Table IV). Protein abundances range from 40 ng/ml to 40 mg/ml. A total of 45 peptides have been described by other groups and deposited in one or both of the plasma databases. Of these 45 peptides that contained the exact TXP epitope of the respective antibody, we were able to identify 19 peptides with ultracentrifugation purification and 13 without. The integration of information from the two growing empirical databases into the published bioinformatical selection algorithm (47) is currently ongoing and will improve the antibody generation process.

One limitation of the TXP workflow with combined ultracentrifugation purification is the time needed for the ultracentrifugation step and the limited capacities of ultracentrifuge rotors. A maximum of 12 samples can be applied with our setup at the same time with the rotor used in this study, requiring a total of 24 h from sample preparation to data output. Centrifugation time could be reduced to less than 2 h by employing the latest generation centrifuge and rotors that allow higher g-forces. Because of parallelization, ultracentrifugation would not require much more time per sample than a conventional

TABLE IV  
 Comparison of peptide sequences identified in TXP immunoaffinity enriched fractions versus peptide sequences found in empirical databases representing the subset of tryptic peptides experimentally shown to be detectable by mass spectrometry  
 Immunoaffinity enriched fractions are in bold type. Protein abundance in human plasma is indicated where known. NK, not known.

Sequence	Molecular mass, Da	Uniprot reference	Protein Atlas Human Plasma	HUPO Plasma Proteome Project	Plasma concentration, µg/ml	Reference
VLLDQLR	855.52	Q9HDC9: Adipocyte plasma membrane-associated protein		IP100031131.2	NK	
<b>VLLDGVQNR</b>	<b>1109.62</b>	<b>P01024: Complement C3</b>	<b>PAp00028461</b>	<b>IP100164623.2</b>	1.3E+03	38
<b>VLLDQLGTTISFER</b>	<b>1590.86</b>	<b>P04114: Apolipoprotein B-100</b>	<b>PAp00028462</b>	<b>IP100022229.1</b>	9.15E+02	39
VLLDWINDVIVVEER	1711.91	Q9HBH1: β-Parvin	PAP00139400		NK	
<b>VELEDWNGR</b>	<b>1116.52</b>	<b>P02679: Fibrinogen γ chain</b>	<b>PAP00045733</b>	<b>IP100021891.3</b>	9.15E+02	39
VELEDVFNGR	1191.55	O75636: Ficolin-3		IP100293925.1	1.5E+01	44
<b>VELEDWAGNEAYAEYHFR</b>	<b>2197.97</b>	<b>P02671: Fibrinogen α chain</b>	<b>PAP00149457</b>		1.25E+03	39
GDAVAFVK	734.40	P02787: Serotransferrin	PAP00161845	IP100022463.1	4.00E+03	45
<b>DGADVAFVK</b>	<b>977.48</b>	<b>P02787: Serotransferrin</b>	<b>PAP00024622</b>	<b>IP100022463.1</b>	4.00E+03	45
<b>QPSAFAAFVK</b>	<b>1151.60</b>	<b>P01024: Complement C3</b>	<b>PAP00027449</b>	<b>IP100032257.1</b>	1.3E+03	38
CLAEGAGDVAFK	1335.63	P08582: Melanotransferrin	PAP00001121		NK	
CLAENAGDVAFK	1392.65	P02788: Lactotransferrin	PAP00064486		2.70E-01	45
DAVERPQEFITVAFVK	1819.97	P04114: Apolipoprotein B-100	PAP00024585	IP100022229.1	9.15E+02	44
<b>IYSHIDAPK</b>	<b>1179.60</b>	<b>P00450: Ceruloplasmin</b>	<b>PAP00044520</b>	<b>IP100017601.1</b>	2.80E+02	38
FFQYDTWK	1133.52	P01344: Insulin-like growth factor II	PAP00137404		4.00E-01	45
HRPELIDYK	1226.64	P12814: α-Actinin 1	PAP00040808		NK	
<b>EFCVESLVSQYFQVTVDYK</b>	<b>2349.06</b>	<b>P02652: Apolipoprotein A-II</b>	<b>PAP00024985</b>	<b>IP100021854.1</b>	2.44E+02	38
<b>VVCSCTEGYR</b>	<b>1229.47</b>	<b>P00740: Coagulation factor IX</b>	<b>PAP00378430</b>	<b>IP100296176.1</b>	4.50E+00	48
DDGSWEVIEGYR	1424.62	P00367: Glutamate dehydrogenase 1, mitochondrial P49448: Glutamate dehydrogenase 2, mitochondrial	PAP00064702		NK	
<b>MDCQCEPGRY</b>	<b>1443.48</b>	<b>P21333: Filamin-A</b>	<b>PAP00026827</b>		NK	
<b>NIPGFCECPGRY</b>	<b>1841.69</b>	<b>P07225: Vitamin K-domain-containing protein S</b>		<b>IP100294004.1</b>	3.50E-02	40
MMHEEHLR	1081.48	O8Y825: Coiled-coil domain-containing protein 135		IP100217687.1	2.50E+01	39
VVNSTTGPGEHLR	1365.70	P07996: Thrombospondin-1	PAP00415875		NK	
<b>SCVGETESTQCEDELEHLR</b>	<b>2508.00</b>	<b>P10643: Complement component C7</b>	<b>PAP00027646</b>	<b>IP100296608.1</b>	2.00E-01	45
APTAQVESFR	1104.56	P24821: Tenascin	PAP00091921		1.00E+00	45
APEENTAAIVYVNGESENQESFR	2682.20	Q8TEP8: Centrosomal protein of 192 kDa		IP100181475.1	NK	
TDMEEVLR	1104.55	P12955: Xaa-Pro dipeptidase	PAP00094413	IP100257982.1	NK	
FLEEHFPGGEVLR	1510.74	P00167: Cytochrome b <sub>5</sub>	PAP00185870		NK	
LLANNPEDPPGSEVLR	1811.91	Q15166: Serum paraoxonase/lactonase 3	PAP00093392	IP100217446.1	NK	
<b>IFFYDSENPFASEVLR</b>	<b>1882.91</b>	<b>P27169: Serum paraoxonase/arylesterase 1</b>	<b>PAP00025909</b>	<b>IP100218732.1</b>	5.93E+01	38
MGDVLLVLDGEEVLR	1888.91	P04278: Sex hormone-binding globulin	PAP00044875	IP100023019.1	6.00E+00	44
<b>YNPVIIDFEMQFIHEVLR</b>	<b>2198.12</b>	<b>P07357: Complement component C8 alpha chain</b>	<b>PAP00039195</b>	<b>IP100011252.1</b>	4.70E+01	39
<b>TPSCGDICNFPFK</b>	<b>1491.61</b>	<b>P04003: C4b-binding protein α chain</b>	<b>PAP00060583</b>	<b>IP100021727.1</b>	3.65E+02	39
EASHVLEVK	1010.54	Q9Y5S2: Serine/threonine-protein kinase MRCK β	PAP00025874	IP100005689.2	NK	
IDDIWNLEVK	1243.64	P04114: Apolipoprotein B-100	PAP00022229.1	IP100022229.1	9.15E+02	44
ALEEANADLEVK	1300.65	P13646: Keratin, type I cytoskeletal 13	PAP00039444	IP100179358.1	NK	
ALEEANTELEVK	1344.68	P02533: Keratin, type I cytoskeletal 14		IP100218819.1	NK	
VFGAPVLENLEVK	1542.83	P19012: Keratin, type I cytoskeletal 15		IP100291755.1	NK	
LSQGEVGEPAFTDPLGLDLDVALSNLEVK	3024.48	P08779: Keratin, type I cytoskeletal 16			NK	
<b>GLPAPIEK</b>	<b>823.48</b>	<b>Q04695: Keratin, type I cytoskeletal 17</b>	<b>PAP00032389</b>	<b>IP100244103.1</b>	NK	
<b>ALPAPIEK</b>	<b>837.50</b>	<b>Q8TEM1: Nuclear pore membrane glycoprotein 210</b>	<b>PAP00074141</b>	<b>IP100004608.1</b>	2.84E+03	39
		<b>Q86UX7: Ferritin chain C region;</b>	<b>PAP00029028</b>	<b>IP100004617.1</b>	4.30E+03	39
		<b>P01857: Ig γ1 chain C region;</b>		<b>IP100152302.1</b>	NK	
		<b>P01860: Ig γ3 chain C region</b>		<b>IP100168728.1</b>	NK	
DAGMQLQGYR	1137.52	P00505: Aspartate aminotransferase, mitochondrial	PAP00131640		NK	
TDGCOHFCLPGQESVTCSCAQGYR	2881.05	P22891: Vitamin K-dependent protein Z	PAP00445892	IP100027843.1	3.00E+00	44
<b>VFQVSTPFLVEVSR</b>	<b>1510.84</b>	<b>P02768: serum albumin</b>	<b>PAP00028510</b>	<b>IP100022434.1</b>	4.10E+04	38
<b>LFDSDFITVTFVVEVSR</b>	<b>1872.98</b>	<b>P10909: Clusterin</b>	<b>PAP00026453</b>	<b>IP100291262.1</b>	1.0E+02	39

nano-LC separation and could represent an attractive and potentially more robust alternative to demanding nanochromatography-based separations.

In conclusion, our study demonstrates the feasibility of enriching several peptides from nondepleted tryptic plasma digests using TXP antibodies targeting groups of peptides sharing a common short (4–5 amino acids) motif. We showed that the in-solution purification of TXP antibody-peptide immunocomplexes from excess nontargeted peptides from whole plasma digests is possible using ultracentrifugation. Incorporation of this additional separation step improved the number of identifiable peptides and increased the sensitivity of the assay to within reach of current multireaction monitoring-based immunoassays without the requirement for complex chromatographic separation.

**Acknowledgments**—We thank Elisabeth Kremmer (Helmholtz Center Munich) for the kind gift of the anti-HA tag antibody.

**Potential Conflict of Interest**—C. W. is the founder of Wellspring Clinical Lab, Inc. (Altamonte Springs, FL). Wellspring develops immunoaffinity-MS assays.

 This article contains [supplemental material](#).

§ These authors contributed equally to this work.

\*\* To whom correspondence should be addressed: NMI Natural and Medical Sciences Institute at the University of Tübingen, Markwiesenstr. 55, 72770 Reutlingen, Germany. Tel.: 49-7121-51530-802; Fax: 49-7121-51530-816; E-mail: poetz@nmi.de.

#### REFERENCES

- Veenstra, T. D., Conrads, T. P., Hood, B. L., Avellino, A. M., Ellenbogen, R. G., and Morrison, R. S. (2005) Biomarkers: Mining the Biofluid Proteome. *Mol. Cell. Proteomics* **4**, 409–418
- Anderson, N. L., and Anderson, N. G. (2002) The human plasma proteome: History, character, and diagnostic prospects. *Mol. Cell. Proteomics* **1**, 845–867
- Jacobs, J. M., Adkins, J. N., Qian, W. J., Liu, T., Shen, Y., Camp, D. G., 2nd, and Smith, R. D. (2005) Utilizing human blood plasma for proteomic biomarker discovery. *J. Proteome Res.* **4**, 1073–1085
- Steel, L. F., Trotter, M. G., Nakajima, P. B., Mattu, T. S., Gonye, G., and Block, T. (2003) Efficient and specific removal of albumin from human serum samples. *Mol. Cell. Proteomics* **2**, 262–270
- Pieper, R., Su, Q., Gatlin, C. L., Huang, S. T., Anderson, N. L., and Steiner, S. (2003) Multi-component immunoaffinity subtraction chromatography: An innovative step towards a comprehensive survey of the human plasma proteome. *Proteomics* **3**, 422–432
- Liu, T., Qian, W. J., Mottaz, H. M., Gritsenko, M. A., Norbeck, A. D., Moore, R. J., Purvine, S. O., Camp, D. G., 2nd, and Smith, R. D. (2006) Evaluation of multiprotein immunoaffinity subtraction for plasma proteomics and candidate biomarker discovery using mass spectrometry. *Mol. Cell. Proteomics* **5**, 2167–2174
- Qian, W. J., Kaleta, D. T., Petritis, B. O., Jiang, H., Liu, T., Zhang, X., Mottaz, H. M., Varnum, S. M., Camp, D. G., 2nd, Huang, L., Fang, X., Zhang, W. W., and Smith, R. D. (2008) Enhanced detection of low abundance human plasma proteins using a tandem IgY12-SuperMix immunoaffinity separation strategy. *Mol. Cell. Proteomics* **7**, 1963–1973
- Gong, Y., Li, X., Yang, B., Ying, W., Li, D., Zhang, Y., Dai, S., Cai, Y., Wang, J., He, F., and Qian, X. (2006) Different immunoaffinity fractionation strategies to characterize the human plasma proteome. *J. Proteome Res.* **5**, 1379–1387
- Seam, N., Gonzales, D. A., Kern, S. J., Hortin, G. L., Hoehn, G. T., and Suffredini, A. F. (2007) Quality control of serum albumin depletion for proteomic analysis. *Clin. Chem.* **53**, 1915–1920
- Gundry, R. L., White, M. Y., Noguee, J., Tchernyshyov, I., and Van Eyk, J. E. (2009) Assessment of albumin removal from an immunoaffinity spin column: Critical implications for proteomic examination of the albuminome and albumin-depleted samples. *Proteomics* **9**, 2021–2028
- Ichibangase, T., Moriya, K., Koike, K., and Imai, K. (2009) Limitation of immunoaffinity column for the removal of abundant proteins from plasma in quantitative plasma proteomics. *Biomed. Chromatogr.* **23**, 480–487
- Wittmann-Liebold, B., Graack, H. R., and Pohl, T. (2006) Two-dimensional gel electrophoresis as tool for proteomics studies in combination with protein identification by mass spectrometry. *Proteomics* **6**, 4688–4703
- Washburn, M. P., Wolters, D., and Yates, J. R., 3rd (2001) Large-scale analysis of the yeast proteome by multidimensional protein identification technology. *Nat. Biotechnol.* **19**, 242–247
- Qian, W. J., Jacobs, J. M., Liu, T., Camp, D. G., 2nd, and Smith, R. D. (2006) Advances and challenges in liquid chromatography-mass spectrometry-based proteomics profiling for clinical applications. *Mol. Cell. Proteomics* **5**, 1727–1744
- Gygi, S. P., Rist, B., Gerber, S. A., Turecek, F., Gelb, M. H., and Aebersold, R. (1999) Quantitative analysis of complex protein mixtures using isotope-coded affinity tags. *Nat. Biotechnol.* **17**, 994–999
- Zhang, H., Li, X. J., Martin, D. B., and Aebersold, R. (2003) Identification and quantification of N-linked glycoproteins using hydrazide chemistry, stable isotope labeling and mass spectrometry. *Nat. Biotechnol.* **21**, 660–666
- Ackermann, B. L., and Berna, M. J. (2007) Coupling immunoaffinity techniques with MS for quantitative analysis of low-abundance protein biomarkers. *Expert Rev. Proteomics* **4**, 175–186
- Anderson, N. L., Anderson, N. G., Haines, L. R., Hardie, D. B., Olafson, R. W., and Pearson, T. W. (2004) Mass spectrometric quantitation of peptides and proteins using stable isotope standards and capture by anti-peptide antibodies (SISCAPA). *J. Proteome Res.* **3**, 235–244
- Whiteaker, J. R., Zhao, L., Anderson, L., and Paulovich, A. G. (2010) An automated and multiplexed method for high throughput peptide immunoaffinity enrichment and multiple reaction monitoring mass spectrometry-based quantification of protein biomarkers. *Mol. Cell. Proteomics* **9**, 184–196
- Kuhn, E., Addona, T., Keshishian, H., Burgess, M., Mani, D. R., Lee, R. T., Sabatine, M. S., Gerszten, R. E., and Carr, S. A. (2009) Developing multiplexed assays for troponin I and interleukin-33 in plasma by peptide immunoaffinity enrichment and targeted mass spectrometry. *Clin. Chem.* **55**, 1108–1117
- Hoofnagle, A. N., Becker, J. O., Wener, M. H., and Heinecke, J. W. (2008) Quantification of thyroglobulin, a low-abundance serum protein, by immunoaffinity peptide enrichment and tandem mass spectrometry. *Clin. Chem.* **54**, 1796–1804
- Poetz, O., Hoeppe, S., Templin, M. F., Stoll, D., and Joos, T. O. (2009) Proteome wide screening using peptide affinity capture. *Proteomics* **9**, 1518–1523
- Wingren, C., James, P., and Borrebaeck, C. A. (2009) Strategy for surveying the proteome using affinity proteomics and mass spectrometry. *Proteomics* **9**, 1511–1517
- Hoeppe, S., Schreiber, T. D., Planatscher, H., Zell, A., Templin, M. F., Stoll, D., Joos, T. O., and Poetz, O. (2010) Targeting peptide termini: A novel immunoaffinity approach to reduce complexity in mass spectrometric protein identification. *Mol. Cell. Proteomics* **10**.1074/mcp.M110.002857
- Anderson, N. L., Jackson, A., Smith, D., Hardie, D., Borchers, C., and Pearson, T. W. (2009) SISCAPA peptide enrichment on magnetic beads using an in-line bead trap device. *Mol. Cell. Proteomics* **8**, 995–1005
- Svedberg, T. (1934) Molecular weight analysis in centrifugal fields. *Science* **79**, 327–332
- Tengerdy, R. P., and Faust, C. H., Jr. (1971) Separation of soluble antigen-antibody complexes by acrylamide gel electrophoresis and ultracentrifugation. *Anal. Biochem.* **42**, 248–254
- Rodahl, E., Iversen, O. J., and Dalen, A. B. (1984) Preparative isolation of immune complexes from serum by sucrose gradient ultracentrifugation. *Scand. J. Immunol.* **20**, 21–26
- Friguet, B., Chaffotte, A. F., Djavadi-Ohanian, L., and Goldberg, M. E. (1985) Measurements of the true affinity constant in solution of antigen-antibody complexes by enzyme-linked immunosorbent assay. *J. Immunol. Methods* **77**, 305–319
- Friguet, B., Chaffotte, A. F., Djavadi-Ohanian, L., and Goldberg, M. E. (1995) Under proper experimental conditions the solid-phase antigen

- does not disrupt the liquid phase equilibrium when measuring dissociation constants by competition ELISA. *J. Immunol. Methods* **182**, 145–150
31. Kurzeder, C., Koppold, B., Sauer, G., Pabst, S., Kreienberg, R., and Deissler, H. (2007) CD9 promotes adeno-associated virus type 2 infection of mammary carcinoma cells with low cell surface expression of heparan sulphate proteoglycans. *Int. J. Mol. Med.* **19**, 325–333
  32. Poetz, O., Luckert, K., Herget, T., and Joos, T. O. (2009) Microsphere-based co-immunoprecipitation in multiplex. *Anal. Biochem.* **395**, 244–248
  33. Jimenez, C. R., El Filali, Z., Knol, J. C., Hoekman, K., Kruyt, F. A., Giaccone, G., Smit, A. B., and Li, K. W. (2007) Automated serum peptide profiling using novel magnetic C18 beads off-line coupled to MALDI-TOF-MS. *Proteomics Clin. Appl.* **1**, 598–604
  34. Haenel, C., Satzger, M., Ducata, D. D., Ostendorp, R., and Brocks, B. (2005) Characterization of high-affinity antibodies by electrochemiluminescence-based equilibrium titration. *Anal. Biochem.* **339**, 182–184
  35. Knochenmuss, R., and Zenobi, R. (2003) MALDI ionization: The role of in-plume processes. *Chem. Rev.* **103**, 441–452
  36. Reid, J. D., Holmes, D. T., Mason, D. R., Shah, B., and Borchers, C. H. (2010) Towards the development of an immuno MALDI (iMALDI) mass spectrometry assay for the diagnosis of hypertension. *J. Am. Soc. Mass Spectrom.* **21**, 1680–1686
  37. Kratzer, R., Eckerskorn, C., Karas, M., and Lottspeich, F. (1998) Suppression effects in enzymatic peptide ladder sequencing using ultraviolet: Matrix-assisted laser desorption/ionization-mass spectrometry. *Electrophoresis* **19**, 1910–1919
  38. Polanski, M., and Anderson, N. L. (2007) A list of candidate cancer biomarkers for targeted proteomics. *Biomark. Insights* **1**, 1–48
  39. Hortin, G. L., Sviridov, D., and Anderson, N. L. (2008) High-abundance polypeptides of the human plasma proteome comprising the top 4 logs of polypeptide abundance. *Clin. Chem.* **54**, 1608–1616
  40. Alper, O., Stetler-Stevenson, W. G., Harris, L. N., Leitner, W. W., Ozdemirli, M., Hartmann, D., Raffeld, M., Abu-Asab, M., Byers, S., Zhuang, Z., Oldfield, E. H., Tong, Y., Bergmann-Leitner, E., Criss, W. E., Nagasaki, K., Mok, S. C., Cramer, D. W., Karaveli, F. S., Goldbach-Mansky, R., Leo, P., Stromberg, K., and Weil, R. J. (2009) Novel anti-filamin-A antibody detects a secreted variant of filamin-A in plasma from patients with breast carcinoma and high-grade astrocytoma. *Cancer Sci.* **100**, 1748–1756
  41. Whiteaker, J. R., Zhao, L., Abbatiello, S. E., Burgess, M., Kuhn, E., Lin, C., Pope, M. E., Razavi, M., Anderson, N. L., Pearson, T. W., Carr, S. A., and Paulovich, A. G. (2011) Evaluation of large scale quantitative proteomic assay development using peptide affinity-based mass spectrometry. *Mol. Cell. Proteomics* **10**.1074/mcp.M110.005645
  42. Stahl-Zeng, J., Lange, V., Ossola, R., Eckhardt, K., Krek, W., Aebersold, R., and Domon, B. (2007) High sensitivity detection of plasma proteins by multiple reaction monitoring of N-glycosites. *Mol. Cell. Proteomics* **6**, 1809–1817
  43. Jiang, J., Parker, C. E., Hoadley, K. A., Perou, C. M., Boysen, G., and Borchers, C. H. (2007) Development of an immuno tandem mass spectrometry (iMALDI) assay for EGFR diagnosis. *Proteomics Clin. Appl.* **1**, 1651–1659
  44. Kovarik, P., Grivet, C., Bourgoigne, E., and Hopfgartner, G. (2007) Method development aspects for the quantitation of pharmaceutical compounds in human plasma with a matrix-assisted laser desorption/ionization source in the multiple reaction monitoring mode. *Rapid Commun. Mass Spectrom.* **21**, 911–919
  45. Deutsch, E. W., Lam, H., and Aebersold, R. (2008) PeptideAtlas: A resource for target selection for emerging targeted proteomics workflows. *EMBO Rep.* **9**, 429–434
  46. Omenn, G. S., States, D. J., Adamski, M., Blackwell, T. W., Menon, R., Hermjakob, H., Apweiler, R., Haab, B. B., Simpson, R. J., Eddes, J. S., Kapp, E. A., Moritz, R. L., Chan, D. W., Rai, A. J., Admon, A., Aebersold, R., Eng, J., Hancock, W. S., Hefta, S. A., Meyer, H., Paik, Y. K., Yoo, J. S., Ping, P., Pounds, J., Adkins, J., Qian, X., Wang, R., Wasinger, V., Wu, C. Y., Zhao, X., Zeng, R., Archakov, A., Tsugita, A., Beer, I., Pandey, A., Pisano, M., Andrews, P., Tammen, H., Speicher, D. W., and Hanash, S. M. (2005) Overview of the HUPO Plasma Proteome Project: Results from the pilot phase with 35 collaborating laboratories and multiple analytical groups, generating a core dataset of 3020 proteins and a publicly-available database. *Proteomics* **5**, 3226–3245
  47. Planatscher, H., Supper, J., Poetz, O., Stoll, D., Joos, T., Templin, M. F., and Zell, A. (2010) Optimal selection of epitopes for TXP-immunoaffinity mass spectrometry. *Algorithms Mol. Biol.* **5**, 28–28
  48. Schenk, S., Schoenhals, G. J., de Souza, G., and Mann, M. (2008) A high confidence, manually validated human blood plasma protein reference set. *BMC Med. Genomics* **1**, 41–41